

## Wire Explosion in Water under High Pressure

A.G. Rousskikh, V.I. Oreshkin, A.Yu. Labetsky, A.V. Shishlov, S.A. Chaikovsky

*Institute of High Current Electronics 2/3 Akademicheskoy Ave., 634055 Tomsk, Russia,  
Phone (3822) 492-133, Fax (3822) 491-677, russ@ovpe2.hcei.tsc.ru*

**Abstract** – This paper reports on experimental and theoretical studies of the transport properties of metals at surrounding medium pressures ranging from several tens of thousands to million atmospheres. The experiments were performed on the IMRI-5 generator operating with a current of up to 0.5 MA and with a current risetime of  $\sim 450$  ns. The load was a wire array consisting of 28 copper wires of diameter  $150\ \mu\text{m}$  arranged on a 16-mm scale and a single  $\text{O}30\text{-}\mu\text{m}$  tungsten wire placed on the axis. The multiwire array was exploded in a liquid dielectric – water. The exploded wire array created a shock wave converging on the axis. The tungsten wire was exploded at the instant the shock wave reached the axis. The shock wave pressure measured at the center of the wire array was at a level of 60-100 kbar. In the experiments, data was gained on the electrical explosion of wires in the fast high-pressure regime at current densities higher than  $10^8\ \text{A}/\text{cm}^2$ . The transport coefficients of metals at high pressures were determined by comparing the experimental findings and the results of MHD simulations of electrically exploded wires.

The simulation of the wire explosion under high pressure using the theoretically obtained transport coefficients shows a good agreement with the experiments.

### 1. Introduction

The electrical explosion of wires (EEW) has long been attractive to researchers [1]. Recent interest in EEW has been provoked chiefly by successful experiments with soft X-rays produced on implosion of cylindrical multiwire arrays on the Angara-5-1 and Z generators [2, 3].

Experiments with EEW provide information on the transport properties of non-ideal plasma, in particular, on the conductivity of matters. From this standpoint, of most interest is EEW in a liquid dielectric, in particular, in water [4, 5], rather than EEW in vacuum, which involves stratoformation, gas desorption from the metal surface, etc., i.e., the processes not directly related to the transport properties of conductors.

The objective of this work is to study the influence of the surrounding medium pressure on the explosion of fine wires in liquid dielectric. The metal to be studied was a tungsten wire of diameter  $30\ \mu\text{m}$  and the liquid dielectric was distilled water. The experiments

were conducted in two stages. At the first stage, we examined the parameters of the converging cylindrical shock wave initiated on explosion of the wire array in water. We determined the instant the shock wave arrived on the system axis and estimated the pressure behind its front from the shock wave velocity. At the second stage, experiments were performed on explosion of the tungsten fine wire in the region of high pressure. The tungsten wire was arranged along the array axis and was exploded at the instant the shock wave arrived on the system axis.

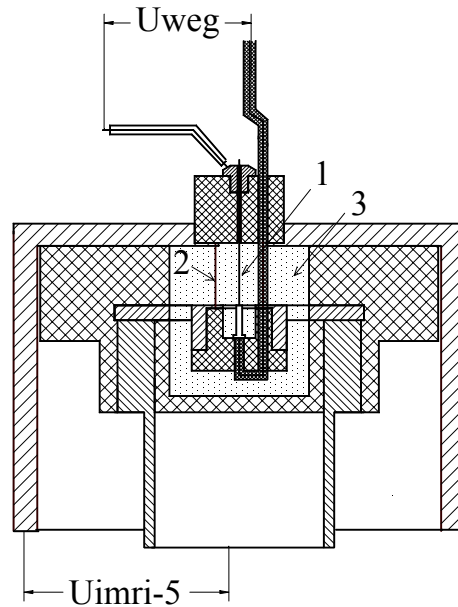


Fig.1. Schematic of the load unit: 1 - W conductor, 2 – multiwire array, 3 – water.

### 2. Explosion of the multiwire array in water

The wire array was exploded in water using the IMRI - 5 pulsed generator [6]. The IMRI - 5 generator is a capacitor bank with a total capacitance  $C_0 = 3.23\ \mu\text{F}$  which are charged to a voltage  $U_0 = 74\ \text{kV}$ . The inductance of the electric circuit is  $70\ \text{nH}$  and the internal resistance of the generator is  $0.15\ \Omega$ . The energy stored in the capacitors is switched to the load region with the use of a multigap trigger. In the short-circuit mode, the generator allows switching currents of amplitude 0.5 MA at a current risetime of 450 ns. A multiwire array consisting of

28 copper wires of diameter 150 μm was used as the load. The diameter and length of the array were 16.3 mm and 2 cm, respectively. Schematic of the load unit is shown in Fig. 1.

The propagation of the shock wave in water was recorded with an optical system [7] using an ISP-250-A flash lamp for illumination. The flash lamp formed a flux of parallel rays in the load region. The brightness of the flash lamp was comparable with that of the glow of the fine wires at the moment of their explosion. The flash flux was imaged at the entrance slit of an optical chronograph FER-7. The time-base was 2.5 μs/cm.

The experiments performed by the foregoing procedure have shown that on explosion of the multiwire array a shock wave is initiated which converges to the system axis within 1.9 ÷ 2.1 μs after the instant the generator IMRI-5 is switched. A chronogram of this process is presented in Fig. 2.

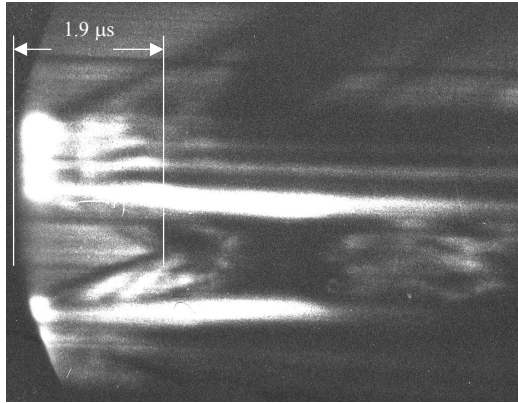


Fig.2 Chronogram of the multiwire array explosion.

Energy equal to the energy of sublimation of the wire array (350 J) is delivered within the first 130 ns of the passage of the IMRI-5 current, whereupon plasma channels with sufficiently low resistance are formed. This allows efficient transfer of the energy of the low-impedance generator into the load. It has been possible to deliver in total an energy of ~7 kJ (~80% of the energy stored in the capacitor bank) to the multiwire array in a time of order 1 μs. On explosion of the wire array, a shock wave with a velocity of  $4.3 \cdot 10^3$  m/s is initiated in water. To estimate the pressure **P** produced by the shock wave, the system of Hugoniot equations [8], which is the law of conservation of mass (1) and the law of conservation of momentum (2) at the shock wave front, should be solved simultaneously with the equation of state of water (3):

$$\rho/\rho_0 = D/(D-U); \quad (1)$$

$$P + \rho \cdot (D-U)^2 = \rho_0 \cdot D^2; \quad (2)$$

$$P = A \cdot ((\rho/\rho_0)^n - 1), \quad (3)$$

where  $\rho_0$  and  $\rho$  are the density of water upstream and downstream of the shock wave front and **D** is the shock wave front velocity, **U** is the mass velocity be-

hind the shock wave front,  $A = 3000$  atm,  $n = 7 \div 8$  [8]. In solving the system of equations (1-3), we obtain that with a shock wave velocity  $D = 4.3 \cdot 10^5$  cm/s the pressure on the system axis  $P = 55 \div 65$  kbar.

### 3. Experiments with a fine wire in the high-pressure region of the converging shock wave

The diameter of the examined tungsten wire, which was located on the axis of the wire array, was 30 μm and its length was 18 mm. This wire was brought into the circuit of the generator WEG [9]. The WEG generator is a 70-nF capacitor bank which is switched by an air trigger. The inductance and the charge voltage of the WEG generator circuit are 1133 nH and 20 kV, respectively. A peculiar feature of the combined use of two separate circuits is that when the IMRI-5 generator circuit draws current a rather high voltage can be induced in the WEG generator. If the induced voltage exceeds the breakdown voltage of the switch in the WEG generator circuit, its premature commutation occurs and synchronization of these two generators becomes impossible.

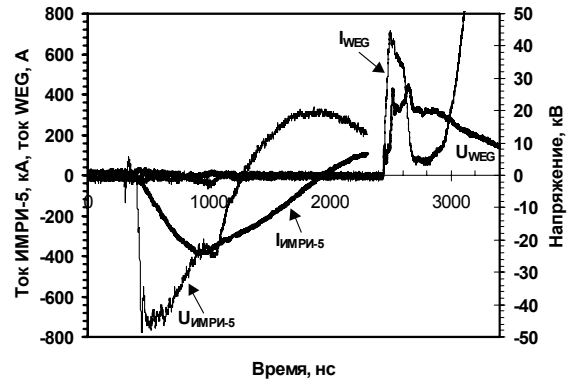


Fig.3 Waveforms of the voltage and current of the IMRI-5 and WEG generators.

This problem was solved by designing the load unit such that the magnetic-flux linkage between the IMRI-5 and WEG generator circuits was minimum. For this purpose, the diameter of the return post of the WEG generator was made coincident with the outer diameter of the wire array (see Fig. 1) and emf of mutual induction in the central conductor is induced only through penetration of the magnetic field into this system.

Figure 3 shows typical waveforms of the synchronous operation of the IMRI-5 and WEG generators. The WEG generator operates at the moment the shock wave is rated to arrive at the center of the system.

In the above geometry, several shots with delays of 1.61, 1.92, 2.05 and 2.26 μs were made. For comparison with the obtained results, calibration shots were made in which only the tungsten wire was exploded

and the shock wave was absent. The greatest difference in the oscillograms of the voltage and current through the exploded wire was found for a shot where the WEG generator operates 2.05  $\mu\text{s}$  later than the IMRI-5 generator. For comparison, Fig. 4 shows oscillograms for the case with and without high pressure on the system axis. It is seen from this figure that with high pressure the fine wire is exploded 15 ns later than without.

Statistical analysis of the experimental data on explosion of tungsten wires on the WEG generator has shown that the spread of moments at which the voltage across the wire peaks is small and is  $\pm 1.5$  ns. Therefore, the obtained experimental dependence of the explosion time of the wire on the surrounding medium pressure may be thought as reliable.

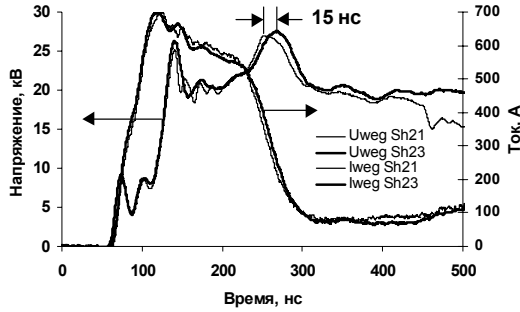


Fig.4. Waveforms of the voltage and current on explosion of the W conductor with ( Sh23 ) and without ( Sh21 ) high pressure in the surrounding medium.

#### 4. Numerical simulation of the EEW in the high-pressure region

To describe the processes occurring on EEW, use was made of the magnetohydrodynamic (MHD) approximation. Numerical calculations in the framework of the MHD approximation require the prior knowledge of the equations of state of matter (EQS) in a wide range of thermodynamic parameters and also the transport factors, of which the most important is conductivity. The EEW was simulated in a one-temperature MHD approximation whose equations in a cylindrical geometry have the form:

$$\frac{d\rho}{dt} + \frac{\rho}{r} \frac{\partial v}{\partial r} = 0; \quad (4)$$

$$\rho \frac{dv}{dt} = -\frac{\partial p}{\partial r} - j_z B_\phi; \quad (5)$$

$$\rho \frac{d\varepsilon}{dt} = -\frac{p}{r} \frac{\partial v}{\partial r} + \frac{j_z^2}{\sigma} + \frac{1}{r} \frac{\partial}{\partial r} r (\kappa \frac{\partial T}{\partial r} - W_R); \quad (6)$$

$$\frac{1}{c} \frac{\partial B_\phi}{\partial t} = \frac{\partial E_z}{\partial r}; \quad j_z = \frac{c}{4\pi r} \frac{\partial (r B_\phi)}{\partial r}; \quad (7)$$

$$j_z = \sigma E_z; \quad (8)$$

$$\varepsilon = f(\rho, T); \quad p = f(\rho, T) \quad (9)$$

where  $\frac{d}{dt} = \frac{\partial}{\partial t} + v \frac{\partial}{\partial r}$  is substantial derivative,

$\rho, T$  are, respectively, the density and temperature of matter,  $v$  is the radial velocity component,  $p, \varepsilon$  are the pressure and the internal energy,  $B_\phi$  the azimuthal component of the magnetic field strength,  $E_z$  is the axial component of the electric field strength,  $j_z$  is the axial component of the current density,  $\kappa, \sigma$  are the thermal conductivity and the conductivity, respectively, and  $W_R$  is the radiation flux.

Equations (4 - 9) were solved numerically with the use of the one-dimensional MHD program EXWIRE [10] written in the Lagrangian coordinates. In this program, hydrodynamic equations (6 - 8) were solved using the explicit difference scheme "cross" [11], in which combined pseudoviscosity (linear and quadratic) was introduced to calculate the shock waves. Maxwell equations (7) complemented by Ohm's law (8) and also the heat equation were solved using implicit difference schemes based on the flow run method [12]. The boundary condition imposed on the Maxwell equations had the form:

$$B_\phi(R) = \frac{2 \cdot I}{c \cdot r_w}, \quad (10)$$

where  $r_w$  is the external, time dependent, radius of a wire and  $I$  is the current through the wire.

The system of MHD equations is completed by equations of state of a matter (9). For the metal, we employed semiempirical wide-aperture equations of state [13] which were based on the model [14] and took into account the effect of high-temperature melting and evaporation. The tungsten conductivity was determined by the computation-experimental procedure [10, 15] in which the conductivity is considered as an empirical function of density and specific energy delivered into a matter.

Two modes of explosion were simulated: with and without high pressure in the water surrounding the tungsten wire. In the first case, the pressure produced on explosion of the multiwire array was simulated by specifying the initial conditions for water. The initial conditions were given with the use of a radial dependence of the water density (linearly ascending to the axis). The water density near the wire surface was 1.6 g/cm<sup>3</sup> that corresponded to a pressure of 65 kbar and at the site of the multiwire array it was 1 g/cm<sup>3</sup>.

Figure 5 shows the calculated current-voltage characteristics for two modes of explosion. It is seen from comparison of the calculated and experimental current-voltage characteristics for these modes of explosion (Figs. 5 and 4) that the influence of the high pressure of the surrounding medium on the characteristics of the explosion is the same in both cases. Namely, the second peak of the voltage (the first peak implies melting of the tungsten wire) on the experi-

mental and calculated waveforms, which corresponds to the moment of explosion, shifts toward longer times.

Thus, the high pressure in the region of the exploded wire causes a delay of the EEW and., hence, an increase in the energy delivered into the metal by the moment of explosion. The good qualitative and quantitative agreement between the experiments and calculations testifies to adequacy of the used theoretical model [10, 15], which describes the transport properties of the imperfect dense plasma of metals.

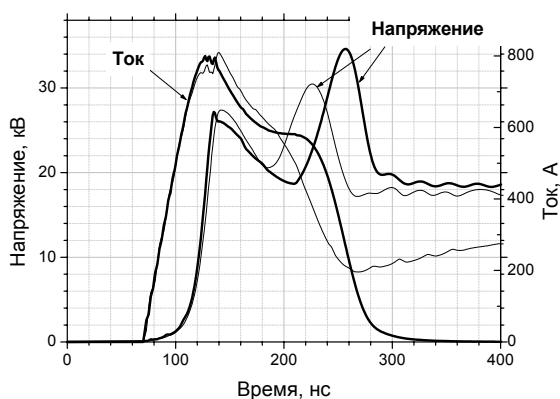


Fig.5 Calculated oscillograms of the voltage and current on explosion of the tungsten conductor with (thick solid lines) and without (thin solid lines) high pressure in the surroundings.

The work was supported by the Russian Foundation for Basic Research, Grant No. 05-02-16845. The authors are grateful to the Russian Science Support Foundation for support of the work done by V.I. Oreshkin and A.V. Shishlov.

## References

- [1] A.A. Rakhudze, *Exploding wires*, Inostran. Liter., Moscow (1959).
- [2] G.S. Volkov, E.V. Grabovsky, K.N. Mitrofanov, G.M. Oleinik, *Plasma Physics*, V. 30, No. 2, p. 99 (2004).
- [3] R.B. Spielman, C. Deeney, G.A. Chandler, et. al., *Phys. of Plasmas* V. 5, No. 5, P. 2105 (1998)
- [4] A.M. DeSilva, J.D. Katsouros, *Phys. Rev.*, E 57, P.6557 (1998).
- [5] A. Grinenko, Ya.E. Krasik, S. Efimov, et.al., *Phys. of Plasmas* 13, 042701 (2006).
- [6] S.A. Chaikovsky, A.Yu. Labetsky, A.V. Shishlov, et.al., – in *AIP Conf. Proc.*, 651. *5th Intern. Conf. on Dense Z-pinch*. – Albuquerque, New Mexico, 2002, pp.123-126.
- [7] A. Grinenko, V.Tz. Gurovich, A. Saypin et.al., *Physical Review E* 72, 066401 (2005).
- [8] Я.Б. Зельдович, Ю.П. Райзер *Физика ударных волн и высокотемпературных гидродинамических явлений*, Москва, Наука, 1966.
- [9] A.G. Rousskikh, R.B. Baksht, S.A. Chaikovsky, et. al., in *Proc. of 13<sup>th</sup> Intern. Symp. on High Current Electronics*, 2004, pp.367-370.
- [10] В.И. Орешкин, Р.Б. Бакшт, А.Ю. Лабетский и др., *ЖТФ*, том 74, вып.7, стр.38-43, (2004).
- [11] Н.Н. Калиткин *Численные методы*, Москва, Наука, 1978, 511стр.
- [12] А.А. Самарский, Ю.П. Попов, *Разностные схемы газовой динамики*, Москва, Наука, 1975.
- [13] С.И. Ткаченко, К.В. Хищенко, В.С. Воробьев и др., *ТВТ*, Т. 39, С.728 (2001).
- [14] A.V. Bushman, V.E. Fortov, *Sov. Tech. Rev. B: Therm. Phys.*, V.1, P.219 (1987).
- [15] Ю.Д. Бакулин, В.Ф. Куропатенко, А.В. Лучинский, *ЖТФ*, Т.20, С.1963 (1976).